Complementarity in which-path resonant Auger scattering

Ji-Cai Liu,[1,2,*] Faris Gel'mukhanov,[3,4] Sergey Polyutov,[4] Pavel Krasnov,[4] and Victor Kimberg[3,†]

[1]*School of Mathematics and Physics, North China Electric Power University, 102206 Beijing, China*

[2]*Hebei Key Laboratory of Physics and Energy Technology, North China Electric Power University, 071000 Baoding, China*

[3]*Division of Theoretical Chemistry and Biology, KTH Royal Institute of Technology, 10691 Stockholm, Sweden*

[4]*International Research Center of Spectroscopy and Quantum Chemistry–IRC SQC, Siberian Federal University, 660041 Krasnoyarsk, Russia*

(Received 30 October 2023; accepted 25 January 2024; published 20 February 2024)

Different types of Young's double-slit experiments contain a significant amount of both particle and wave information running from full-particle to full-wave knowledge depending on the experimental conditions. We study the Young's double-slit interference in resonant Auger scattering from homonuclear diatomic molecules where opposite Doppler shifts for the dissociating atomic slits provide path information. Different quantitative formulation of Bohr's complementarity principle—path information vs interference—is applied to two types of resonant Auger scattering experiments, with fixed-in-space and randomly oriented molecules. Special attention is paid to the orientational dephasing in conventional Auger experiments with randomly oriented molecules. Our quantitative formulation of the complementarity is compared with the formulation made earlier by Greenberger and Yasin [D. M. Greenberger and A. Yasin, Phys. Lett. A **128**, 391 (1988)].

DOI: 10.1103/PhysRevA.109.023116

I. INTRODUCTION

Bohr's complementarity principle [1] asserts that objects have certain pairs of complementary properties or observables which cannot be obtained simultaneously. The general complementarity was invoked by Bohr to preserve wave-particle duality. The special case of general complementarity is the Heisenberg uncertainty principle [2] for such pairs as momentum-coordinate and angular momentum-angle. The key feature of quantum mechanics is the interference which was first observed in optics by Young in his seminal Young's double-slit experiment (YDSE) [3]. Later the YDSE interference of x-ray photons or photoelectrons was studied and observed in many experiments with molecules [4–10]. Similar YDSE fringes were observed also for interfering atoms and molecules (so-called matter wave interference) [11,12]. The complementarity or duality principle says that the YDSE fringes must disappear if the path taken by the particle is experimentally determined [1]. Greenberger and Yasin (GY) [13] discussing the complementarity between interference (INT) and which-path information (WPI) formulated and quantified one of the crucial outcomes of the Bohr-Einstein discussion [1] that it is impossible to have a maximum visibility of interference pattern and path information at the same time. Further deep extensions and refinements of this complementarity were done by Englert [14] (see also Refs. [15–18] and references therein).

However, the quantitative formulation of the discussed complementarity is not unique. For example, there is an experimental situation where the GY path information is strictly equal to zero in spite of the path taken by the particle being experimentally determined. This is the case of the resonant Auger scattering (RAS) by the O_2 molecule where the "atomic slits" are distinguished due to the opposite Doppler labeling of the atomic slits. Thus, one of the goals of our article is to give an alternative quantitative formulation of the WPI-INT complementarity principle which overcomes this drawback. Our article is devoted to a rather frequent situation when the external path-detector is absent. For example, this is the case of the here analyzed RAS experiment with the O_2 molecule where the which-path information is offered by nature itself via the Doppler labeling of the atomic slits [19,20]. The wave-particle duality for the YDSE problem taking into account the external path-detectors was studied in Refs. [14,15,17,18].

Another objective of our article is to apply our and GY's formulations of the complementarity principle between the WPI and the INT to two types of RAS by diatomic molecules where the two core-excited atoms play the role of the double slit. The first one is the RAS experiment with fixed-in-space molecules [19,21] which is the first experimental realization of an analog of the Einstein-Bohr recoiling double-slit gedanken experiment at the molecular level [19,20]. The analysis of the second type of RAS experiment [22] performed with randomly oriented oxygen molecules allows us to shed light on the role of the orientational dephasing on the studied duality relation.

The paper is organized as follows. In Sec. II, we present general analysis and quantitative formulation of the complementarity relation for which-path information and

*jicailiu@ncepu.edu.cn

†kimberg@kth.se

interference. The general theory is applied in Sec. III to the Einstein-Bohr recoiling double-slit gedanken experiment at the molecular level with fixed-in-space oxygen molecules. The role of the orientational dephasing in the RAS of randomly oriented molecules is studied in Sec. IV. Our findings are summarized in Sec. V. We use atomic units (a.u.) throughout the text if it is not specified.

II. DUALITY RELATION—INTERFERENCE VS WHICH-PATH INFORMATION—FOR DOUBLE-SLIT EXPERIMENT WITH FIXED-IN-SPACE MOLECULEs

We consider the general case of the scattering of the light or electrons on two slits. It can be the resonant inelastic x-ray scattering [19,23] or the resonant Auger scattering [19,20] described below. The scattering amplitude is the sum of the scattering amplitudes on the right (R) and left (L) slits,

$$F = F_{\rm R} + F_{\rm L}, \quad F_{\rm L}^* F_{\rm R} = |F_{\rm R}||F_{\rm L}|e^{{\rm i}\Phi},$$

where Φ is the phase difference between the two paths. The total intensity of the scattered wave reads

$$\begin{aligned}|F|^2 &= |F_{\rm R} + F_{\rm L}|^2 = |F_{\rm R}|^2 + |F_{\rm L}|^2 + 2{\rm Re}(F_{\rm L}^* F_{\rm R}) \\ &= |F_{\rm R}|^2 + |F_{\rm L}|^2 + 2|F_{\rm R}||F_{\rm L}|\cos\Phi.\end{aligned}$$

The last term on the right-hand side of this equation describes the interference between two paths while $|F_{\rm R}|^2 + |F_{\rm L}|^2$ is the intensity of the wave passed independently through two slits. Apparently, when $|F_{\rm R}| = |F_{\rm L}|$, one cannot distinguish which path the particle has traversed. Therefore, it is natural to define the which-path information by the following positive probability:

$$\mathcal{W} = \frac{(|F_{\rm R}| - |F_{\rm L}|)^2}{|F_{\rm R}|^2 + |F_{\rm L}|^2}. \tag{1}$$

The complementary term to the path information ($\mathcal{W}$) is the interference ($\mathcal{I}$), which we define after Greenberger and Yasin [13] as follows:

$$\mathcal{I} = \mathcal{I}_0|\cos\Phi| = \frac{2|{\rm Re}(F_{\rm R}^* F_{\rm L})|}{|F_{\rm R}|^2 + |F_{\rm L}|^2}, \ \mathcal{I}_0 = \frac{2|F_{\rm R}||F_{\rm L}|}{|F_{\rm R}|^2 + |F_{\rm L}|^2}, \tag{2}$$

where $\mathcal{I}_0$ is the contrast or visibility of the interference pattern (fringe visibility) [13]. The complimentarity relation for the WPI and the fringe visibility ($\mathcal{I}_0$) is the equality for the pure quantum states,

$$\mathcal{W} + \mathcal{I}_0 = 1. \tag{3}$$

The complementary or duality relation between $\mathcal{W}$ and $\mathcal{I}$ for pure quantum states reads

$$\mathcal{W} + \mathcal{I} = 1 - \mathcal{I}_0(1 - |\cos\Phi|) \leqslant 1. \tag{4}$$

The complementarity relations (4) and (3) show that the more we know the which-path information the less visible the interference is, and vice versa. It is instructive to compare our definition of the which-path information with the which-path information definition (distinguishability $\mathcal{D}_Q$) of Ref. [17]. The authors of this article studied the problem taking into account external path-detectors characterized by the normalized states $|d_{\rm R}\rangle$ and $|d_{\rm L}\rangle$. Applying the results of Ref. [17] to our case without external path-detectors ($\langle d_{\rm R}|d_{\rm L}\rangle = 1$ [17]),

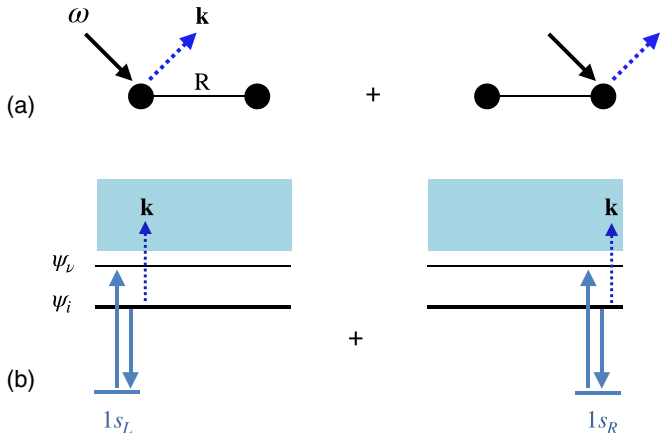

FIG. 1. Scheme of resonant Auger scattering from a homonuclear diatomic molecule. Core excitation $1s_{\rm R/L} \to \psi_\nu$ is followed by the decay transition from an occupied molecular orbital $\psi_i \to 1s_{\rm R/L}$ and emission of an Auger electron with momentum **k**.

we obtained a rather strange result that $\mathcal{D}_Q = 0$ and $\mathcal{D}_Q = \mathcal{W}$ depending on the ratio $|F_{\rm R}|/|F_{\rm L}|$. This disagreement with our Eq. (1) shows that the equations of Ref. [17] are inapplicable to the case studied here of YDSE without path-detectors.

To make the picture complete we give also the GY duality relationship [13] based on the squared probabilities. These authors use an alternative definition of the WPI,

$$\mathcal{W}_{\rm GY} = \frac{||F_{\rm R}|^2 - |F_{\rm L}|^2|}{|F_{\rm R}|^2 + |F_{\rm L}|^2}, \tag{5}$$

which also is equal to zero when $|F_{\rm R}| = |F_{\rm L}|$. The identity $\mathcal{W}_{\rm GY}^2 = 1 - \mathcal{I}_0^2$ allows one to immediately write down GY's duality for the WPI and the fringe visibility [13]:

$$\mathcal{W}_{\rm GY}^2 + \mathcal{I}_0^2 = 1. \tag{6}$$

This together with Eq. (5) results in the GY complimentary inequality for the WPI and the interference:

$$\mathcal{W}_{\rm GY}^2 + \mathcal{I}^2 = 1 - \mathcal{I}_0^2(1 - \cos^2\Phi) \leqslant 1. \tag{7}$$

Although duality relations (4) and (7) have different forms, they are qualitatively the same, except for the process discussed in Sec. IV.

Below we quantify and illustrate the physics behind each of these duality relations for the RAS of the O_2 molecule. The RAS process studied here consists of the resonant x-ray excitation to a dissociative core-excited state, followed by Auger decay to the final dissociative state with emission of a fast Auger electron [19] (Fig. 1).

III. RESONANT AUGER SCATTERING FROM FIXED-IN-SPACE MOLECULES

Detection of the Auger electron with the energy $E = k^2/2$ and the momentum **k** in coincidence with the dissociating ion (Fig. 2) allows one to study the YDSE interference in fixed-in-space molecules with the molecular axis **R** oriented along the velocity **v** of the ion [20,24,25].

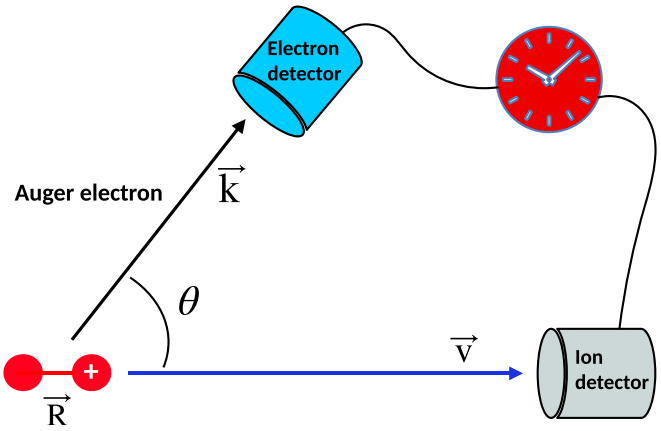

FIG. 2. Experimental setup that registers the Auger electron and the fragmented ion in coincidence (from the same event) allows one to measure RAS spectra from fixed-in-space diatomic molecules [20,25].

A. Doppler labeling of the atomic slits

Let us analyze RAS process with dissociative core-excited and final states (see Fig. 3). This scenario is realized, for example, in RAS from O_2 under core excitation to a dissociative $|O1s^{-1}\sigma^*\rangle$ state [19,20,22]. For studied here homonuclear diatomic molecules RAS amplitude is the sum of the partial scattering amplitudes through the "left" (L) and "right" (R) atoms [19,26] (see Fig. 1)

$$F = F_{\rm L} + \mathcal{P}_f F_{\rm R},$$
$$F_{\rm R,L} = (\mathbf{e}\cdot\mathbf{d}_{0c}) Q_{cf} \int dp_c \frac{\langle 0|\psi_{p_c}\rangle\langle\psi_{p_c}|e^{\pm ikR\cos\theta/2}|\psi_{p_f}\rangle}{E-\omega_{cf}^{\infty}-(\epsilon_{p_c}-\epsilon_{p_f})+i\Gamma}, \tag{8}$$

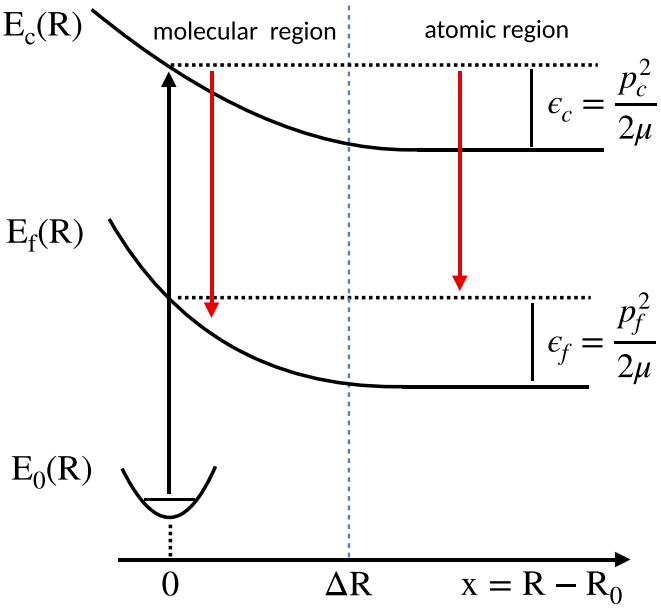

FIG. 3. Schematic representation of the RAS process via dissociative PECs of the core-excited $E_c(R)$ and final $E_f(R)$ states.

where $\mathcal{P}_f = \pm 1$ is the parity of the final state of the molecular cation; Γ is the lifetime broadening of the core-excited state. The prefactor $(\mathbf{e}\cdot\mathbf{d}_{0c})$ describes absorption of x-ray photon with the polarization vector $\mathbf{e}$ in the course of the x-ray core-excitation with the transition dipole moment $\mathbf{d}_{0c}$. The Auger decay is determined by the atomic Coulomb matrix element Q_{cf} of the transition from the core-excited (c) to the final (f) electronic state. The nuclear wave functions $\psi_{p_c}(x)$ and $\psi_{p_f}(x)$ of the dissociative core-excited and final states depend on the nuclear momenta p_c and p_f and internuclear distance R relative to the equilibrium one R_0, $x = R - R_0$. The nuclear momenta $(p_c,\ p_f)$ and kinetic energies $(\epsilon_{p_c} = p_c^2/2\mu,\ \epsilon_{p_f} = p_f^2/2\mu)$ are defined in the asymptotic region $x > \Delta R \sim 0.5$ a.u., where the dissociative potential energy curves (PECs) of the core-excited and final states are already flat (see Fig. 3); $\mu = m/2$ is the reduced mass, $\omega_{cf}^{\infty} = E_c(\infty) - E_f(\infty)$, $E_c(\infty)$ and $E_f(\infty)$ are the asymptotic values of the potential energy at $R \to \infty$.

The phase factors $\exp(\pm i\mathbf{k}\cdot\mathbf{R}/2) = \exp(\pm ikR\cos\theta/2)$, arising from the wave function of the fast Auger electron, indicate opposite phase shifts of the wave functions of the Auger electrons ejected from the "right" and "left" atoms, the signs $+/-$ correspond to the R/L atoms, respectively. Here $\theta = \angle(\mathbf{k},\mathbf{R})$ is the angle between the momentum of the Auger electron $\mathbf{k}$ and internuclear radius vector $\mathbf{R}$. This phase shift is crucial for the YDSE interference. The Franck-Condon (FC) amplitudes $\langle 0|\psi_{p_c}\rangle$ and

$$\langle\psi_{p_c}|e^{\pm ikR\cos\theta/2}|\psi_{p_f}\rangle = e^{\pm ikR_0\cos\theta/2}\langle\psi_{p_c}(x)|e^{\pm ikx\cos\theta/2}|\psi_{p_f}(x)\rangle$$

correspond to the x-ray excitation and Auger decay, respectively [26,27]. In Eq. (8) and below we neglect the momentum of x-ray photon $\mathbf{k}_{\rm ph}$ which is small in the soft x-ray range addressed here. We also neglected a small molecular-field splitting of the core shell, which was found to be important in certain cases, leading to a special regime of resonant x-ray scattering, the so-called nonlocal x-ray scattering [9].

The continuum nuclear wave function of a dissociative state can be represented as the sum

$$\psi_{p_i}(x) = \frac{e^{i(p_i x+\phi)}}{\sqrt{2\pi}} + \varphi_{p_i}(x), \quad i = c, f, \tag{9}$$

of the plane wave and the function $\varphi_{p_i}(x)$ which describes the deviation of the strict wave function $\psi_{p_i}(x)$ from the plane wave. In what follows we omit the phase ϕ [26], which does not affect the "atomic" cross section.

Evidently $\varphi_{p_i}(x) = 0$ in the region $x > \Delta R$ where PECs of the core-excited and final states are flat. Using Eq. (9), one can see that the FC amplitude of the Auger decay consists of a narrow part and a broad ($A_{\rm mol}$) part

$$\langle\psi_{p_c}(x)|e^{\pm ikx\cos\theta/2}|\psi_{p_f}(x)\rangle = \delta\left(p_f \pm \frac{k}{2}\cos\theta - p_c\right) + A_{\rm mol}(p_c, p_f). \tag{10}$$

The first describes the momentum and energy conservation law

$$p_c = p_f \pm \frac{k}{2}\cos\theta, \quad \epsilon_{p_c} - \epsilon_{p_f} \approx \pm kv\cos\theta, \tag{11}$$

where we neglect a small recoil energy $[(k/2)\cos\theta]^2/2\mu$ and introduce the velocity of the dissociating atom in the asymptotic region, $v = p_f/2\mu$. According to Eq. (10) the RAS process is naturally divided into two regions, $x < \Delta R$ and $x > \Delta R$, which are responsible for the formation of a broad "molecular" band and narrow "atomic" (or "fragment") peak, respectively [19,28] (Fig. 3). It is worthwhile noticing that the atomic peak and the molecular band are usually separated in the energy domain and have different dispersion laws [19,21,28]. The Auger electron energy of the molecular band approximately follows the Raman dispersion law, while the peak position of the atomic peak does not depend on the photon energy ω.

The partial RAS amplitudes $F_{\rm R}^{(\rm mol)}$ and $F_{\rm L}^{(\rm mol)}$ of the molecular band differ from each other only by the YDSE phase [20] $F_{\rm R/L}^{(\rm mol)} \propto \exp(\pm {\rm i}[kR_0\cos\theta]/2)$. This results in a nicely resolved YDSE fringe [20]:

$$\sigma_{\rm mol} = \left|F_{\rm R}^{(\rm mol)} + \mathcal{P}_f F_{\rm L}^{(\rm mol)}\right|^2 \propto 1 + \mathcal{P}_f\cos(kR_0\cos\theta). \tag{12}$$

Contrary to the broad molecular band, the atomic peak formed by the δ function in Eq. (10) is split because of the opposite Doppler shifts for the right and left dissociating atoms (11):

$$F_{\rm R/L}^{(\rm at)} = (\mathbf{e}\cdot\mathbf{d}_{0c})\mathcal{Q}_{cf}\frac{\langle 0|\psi_{p_f}\rangle e^{\pm {\rm i}kR_0\cos\theta/2}}{\Delta E \mp kv\cos\theta + {\rm i}\Gamma}. \tag{13}$$

This so-called Auger Doppler effect was predicted earlier [26]. Here $\Delta E = E - \omega_{cf}^{\infty}$ is the energy of the Auger electron with respect to the center of Doppler-split atomic peak ω_{cf}^{∞}. In contrast to the molecular band ($\mathcal{W} = 0$) the opposite Doppler labeling of the right and left atomic slits brings the which-path information $\mathcal{W}$ (1):

$$\left|F_{\rm L}^{(\rm at)}\right| \neq \left|F_{\rm R}^{(\rm at)}\right|, \quad \mathcal{W} \neq 0.$$

This motivates us to focus below on the analysis of the complementarity for the atomic peak. As one can see from Eq. (11) the origin of the Doppler shift is the momentum exchange between the Auger electron and the left or right atom. Due to this, the effect studied here can be considered as a realization of the Einstein-Bohr recoiling double-slit gedanken experiment at the molecular level [19,20] where the left and right paths have opposite Doppler labels.

It is enlightening to write down the cross section for the atomic peak [20,22,26]:

$$\begin{aligned}
\sigma_{\rm at} &= \left|F_{\rm L}^{(\rm at)} + \mathcal{P}_f F_{\rm R}^{(\rm at)}\right|^2 = \sigma_{\rm dir} + \mathcal{P}_f\sigma_{\rm int},\\
\sigma_{\rm dir} &= \left|F_{\rm R}^{(\rm at)}\right|^2 + \left|F_{\rm L}^{(\rm at)}\right|^2,\\
\sigma_{\rm int} &= 2{\rm Re}\left(F_{\rm R}^{(\rm at)}F_{\rm L}^{(\rm at)*}\, e^{{\rm i}kR\zeta}\right),
\end{aligned} \tag{14}$$

with the following expressions for the partial RAS amplitudes:

$$\begin{aligned}
F_{\rm R}^{(\rm at)} &= \frac{(\mathbf{e}\cdot\hat{\mathbf{d}}_{0c})\, e^{{\rm i}kR\zeta/2}}{\Delta E - kv\zeta + {\rm i}\Gamma}, \quad \zeta = \cos\theta,\\
F_{\rm L}^{(\rm at)} &= \frac{(\mathbf{e}\cdot\hat{\mathbf{d}}_{0c})\, e^{-{\rm i}kR\zeta/2}}{\Delta E + kv\zeta + {\rm i}\Gamma},
\end{aligned} \tag{15}$$

where a prefactor $\eta = d_{0c}^2\mathcal{Q}_{cf}^2|\langle 0|\psi_{p_f}\rangle|^2$ is omitted and $\hat{\mathbf{d}} = \mathbf{d}/d$ is the unit vector along $\mathbf{d}$. The probability to pass independently through the left and right atomic slits is described by the direct term $\sigma_{\rm dir}$. The interference term shows clearly the suppression of the visibility of the YDSE pattern by the opposite Doppler shifts which bring the WPI, $|F_{\rm R}^{(\rm at)}| \neq |F_{\rm L}^{(\rm at)}|$, except the ejection of the Auger electron perpendicular to the molecular axis, $\cos\theta \neq 0$.

B. Path information and interference for resonant Auger scattering from fixed-in-space diatomic molecules

Let us analyze the RAS electron-ion coincidence experiment which gives a unique opportunity to study WPI-INT complementarity in the fixed-in-space molecule as the function of the angle $\theta = \angle(\mathbf{k}, \mathbf{R})$ between the momentum of the Auger electron and the molecular axis. Equations (14) and (15) provide the following equations for our and GY's definitions of the which-path information [see Eqs. (1) and (5)] and expressions for the contrast of the interference fringe $\mathcal{I}_0$ and the interference $\mathcal{I}$ (2):

$$\begin{aligned}
&\mathcal{W} = 1 - \mathcal{I}_0, \quad \mathcal{W}_{\rm GY} = \frac{2|D\Delta E|}{(\Delta E)^2 + D^2 + \Gamma^2},\\
&\mathcal{I}_0 = \sqrt{1 - \left(\frac{2D\Delta E}{(\Delta E)^2 + D^2 + \Gamma^2}\right)^2}, \quad \mathcal{I} = \mathcal{I}_0|\cos\Phi|.
\end{aligned} \tag{16}$$

These quantities depend on the Doppler shift (D) and the total phase shift (Φ) which is the sum of the YDSE phase shift ($kR_0\cos\theta$) and the Doppler phase shift (ψ):

$$\begin{aligned}
&D = kv\cos\theta, \quad \Phi = kR_0\cos\theta + \psi,\\
&\tan\psi = \frac{2D}{\Gamma} = \frac{2kv\cos\theta}{\Gamma}.
\end{aligned} \tag{17}$$

To illustrate our duality relations (4) and (3) in comparison with GY relations (7) and (6), we apply Eqs. (16) for the O_2 molecule using here and below the following parameters: $\Gamma = 0.07$ eV, $kv = 0.5$ eV, and $kR_0 = 13.75$, corresponding to the Auger electron kinetic $E \approx 492$ eV. As one can see from Eq. (16), the which-path information is absent ($\mathcal{W} = \mathcal{W}_{\rm GY} = 0$) when the Doppler label of the atomic slit is equal to zero ($D = kv\cos\theta = 0$) or $\Delta E = 0$. The former case takes place for the molecular band [19,20], see Eq. (12), or when the Auger electron is ejected perpendicular to the molecular axis, $\theta = 0$.

Let us first consider the case $\Delta E = 0$. The duality relations (4) and (3) introduced in this paper and ones of GY [Eqs (7) and (6)] are shown in Figs. 4 and 5, respectively, and display qualitatively the same results. Since the which-path information is absent ($\mathcal{W} = 0$, $\mathcal{W}_{\rm GY} = 0$), $\mathcal{I}$ and $\mathcal{W} + \mathcal{I}$ ($\mathcal{I}^2$ and $\mathcal{W}_{\rm GY}^2 + \mathcal{I}^2$) coincide with each other and show the modulation given by ($|\cos\Phi|$, $\cos^2\Phi$) in an agreement with the inequalities $\mathcal{W} + \mathcal{I} \leqslant 1$ (4) and $\mathcal{W}_{\rm GY}^2 + \mathcal{I}^2 \leqslant 1$ (7). The complementarity relations based on the fringe visibility $\mathcal{I}_0$ satisfy equations $\mathcal{W} + \mathcal{I}_0 = 1$ (3) and $\mathcal{W}_{\rm GY}^2 + \mathcal{I}_0^2 = 1$ (6), as illustrated in Figs. 4 and 5.

Now let us consider the strict resonance with one Doppler-shifted atomic slit $\Delta E = kv\cos\theta$ and, hence, the other one is out of resonance. In this case the path information (16) is not equal to zero except for $\theta = \pi/2$ where the Doppler label $D = kv\cos\theta = 0$ and thus $\mathcal{W} = \mathcal{W}_{\rm GY} = 0$. When the Doppler shift approaches the maximum at $\theta = 0$ and π, the

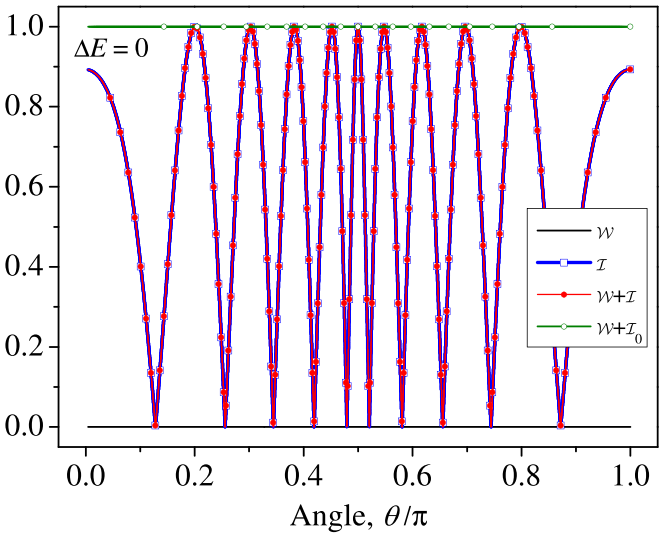

FIG. 4. The complementarity relations based on the WPI definition $\mathcal{W}$ (1) introduced in this paper for the fixed-in-space molecules and $\Delta E = 0$ (energy of the Auger electron E corresponds to the middle of the Doppler doublet). In this case the WPI is absent, $\mathcal{W} = 0$ (16), and the fringe visibility $\mathcal{I}_0$ takes the maximum, $\mathcal{I}_0 = \mathcal{I}_0 + \mathcal{W} = 1$ [Eqs. (2) and (3)]. The interferences $\mathcal{I} = \mathcal{I}_0|\cos\Phi|$ and $\mathcal{I} + \mathcal{W}$ experience oscillations between 0 and 1 as functions of the ejection angle $\theta = \angle(\mathbf{k}, \mathbf{R})$ in agreement with the duality relation (4).

WPI takes the maximum (Figs. 6 and 7) as follows:

$$\mathcal{W}^{\max} = 1 - \frac{\Gamma\sqrt{4(kv)^2 + \Gamma^2}}{2(kv)^2 + \Gamma^2},$$
$$\mathcal{W}_{\rm GY}^{\max} = \frac{2(kv)^2}{2(kv)^2 + \Gamma^2}. \tag{18}$$

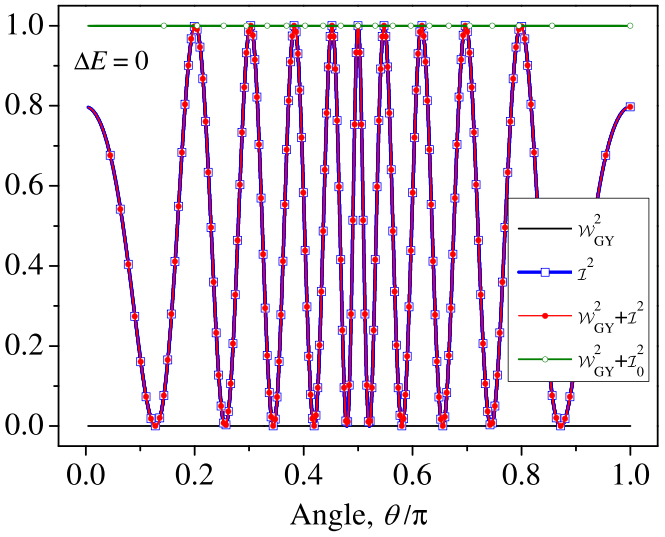

FIG. 5. Same as Fig. 4, but using the complementarity relations based on GY's WPI definition $\mathcal{W}_{\rm GY}$ (5). Similar to Fig. 4, $\mathcal{W}_{\rm GY} = 0$ (16), the fringe visibility takes the maximum $\mathcal{I}_0^2 = \mathcal{I}_0^2 + \mathcal{W}_{\rm GY}^2 = 1$ [Eqs. (2) and (6)], and $\mathcal{I}^2 = \mathcal{I}_0^2\cos\Phi^2$ and $\mathcal{I}^2 + \mathcal{W}_{\rm GY}^2$ oscillate between 0 and 1 as the function of the ejection angle θ (7).

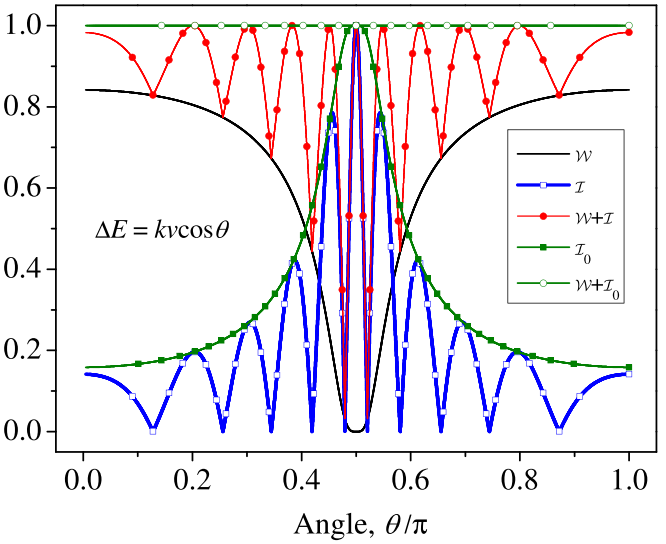

FIG. 6. Same as Fig. 4, but for case when the Auger electron kinetic energy follows the Doppler ridge of the "right" atom, $\Delta E = kv\cos\theta$. Simulations are performed using Eqs. (16).

The maximum of the WPI is smaller than 1, due to the energy uncertainty given by the finite width Γ of the resonance. In full agreement with the duality relations (3) and (6), the fringe visibility $\mathcal{I}_0$ displays exactly opposite θ dependence as compared to $\mathcal{W}$ (Fig. 6) and $\mathcal{W}_{\rm GY}$ (Fig. 7). The interference $\mathcal{I}$ ($\mathcal{I}^2$) oscillates between $\mathcal{I}_0$ ($\mathcal{I}_0^2$) and zero. In an agreement with the complementary relations (4) and (7), the sums $\mathcal{W} + \mathcal{I}$ and $\mathcal{W}_{\rm GY}^2 + \mathcal{I}^2$ do not exceed 1.

IV. RESONANT AUGER SCATTERING BY RANDOMLY ORIENTED MOLECULES: ORIENTATIONAL DEPHASING

In the previous section we investigated the RAS from the fixed-in-space molecule [20,25], which constitutes the

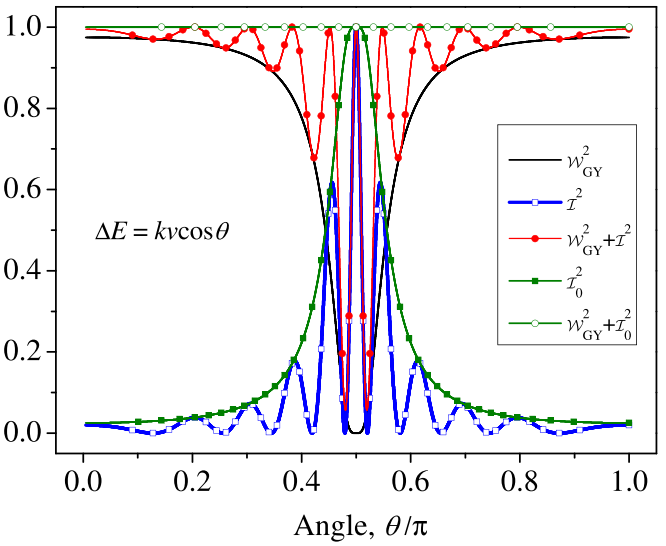

FIG. 7. Same as Fig. 5, but for case when the Auger electron kinetic energy follows the Doppler ridge of the "right" atom, $\Delta E = kv\cos\theta$. Simulations are performed using Eqs. (16).

fully coherent scattering process by the perfectly aligned molecule. However, common RAS experimental setups address randomly oriented ensembles of free molecules [19,22]. In this case, both the Doppler shift $(\mathbf{k}\cdot\mathbf{v})$ and the YDSE fringe $[\exp(i\mathbf{k}\cdot\mathbf{R})]$ fluctuate due to random orientations of the molecular axis $\mathbf{R}$ in the gas phase. In spite of the random orientation of $\mathbf{R}$, a partial selectivity of the absorption transition dipole moment $\mathbf{d}_{0c}$ along the polarization vector $\mathbf{e}$ is still present due to the polarization prefactor $(\mathbf{e}\cdot\mathbf{d}_{0c})$ in Eq. (13). Following the RAS experiment with gas-phase oxygen molecules [22], we assume here that the Auger electron is ejected along the polarization vector $(\mathbf{k}\parallel\mathbf{e})$ and that the x-ray photon frequency is tuned in resonance with the O $1s\rightarrow\sigma^*$ transition to the dissociative core-excited state [19,22]. For this transition $\mathbf{d}_{0c}\parallel\mathbf{R}$, and thus $(\mathbf{e}\cdot\mathbf{d}_{0c})\propto(\mathbf{k}\cdot\mathbf{R})\propto\cos\theta$.

Now we are in the stage of modifing the definition of the which-path information [Eqs. (1) and (5)] and of the interference (2) for the discussed RAS experiment [22] with the randomly oriented oxygen molecules:

$$\begin{aligned}\overline{\mathcal{W}} &= \frac{\left\langle\left(\left|F_{\rm R}^{\rm (at)}\right|-\left|F_{\rm L}^{\rm (at)}\right|\right)^2\right\rangle}{\left\langle\left|F_{\rm R}^{\rm (at)}\right|^2+\left|F_{\rm L}^{\rm (at)}\right|^2\right\rangle} = 1-\frac{2\left\langle\left|F_{\rm R}^{\rm (at)}\right|\left|F_{\rm L}^{\rm (at)}\right|\right\rangle}{\left\langle\left|F_{\rm R}^{\rm (at)}\right|^2+\left|F_{\rm L}^{\rm (at)}\right|^2\right\rangle},\\ \overline{\mathcal{W}}_{\rm GY} &= \frac{\left\langle\left(\left|F_{\rm R}^{\rm (at)}\right|^2-\left|F_{\rm L}^{\rm (at)}\right|^2\right)\right\rangle}{\left\langle\left|F_{\rm R}^{\rm (at)}\right|^2+\left|F_{\rm L}^{\rm (at)}\right|^2\right\rangle},\\ \overline{\mathcal{I}} &= \frac{\left\langle 2\left|{\rm Re}\left(F_{\rm L}^{\rm (at)*}F_{\rm R}^{\rm (at)}\right)\right|\right\rangle}{\left\langle\left|F_{\rm R}^{\rm (at)}\right|^2+\left|F_{\rm L}^{\rm (at)}\right|^2\right\rangle}, \quad \langle f\rangle=\int_{-1}^{1}f(\zeta)d\zeta,\end{aligned} \tag{19}$$

where the angle brackets denote the averaging over orientation. According to Eqs. (14)–(15),

$$\begin{aligned}\left|F_{\rm R}^{\rm (at)}\right| &= \frac{|\zeta|}{\sqrt{(\Delta E-kv\zeta)^2+\Gamma^2}},\\ \left|F_{\rm L}^{\rm (at)}\right| &= \frac{|\zeta|}{\sqrt{(\Delta E+kv\zeta)^2+\Gamma^2}},\ \left|{\rm Re}\left(F_{\rm L}^{\rm (at)*}F_{\rm R}^{\rm (at)}\right)\right|\\ &= \frac{\zeta^2\left|[\Delta E^2+\Gamma^2-(kv\zeta)^2]\cos(kR\zeta)+2\Gamma kv\zeta\,\sin(kR\zeta)\right|}{[(\Delta E-kv\zeta)^2+\Gamma^2][(\Delta E+kv\zeta)^2+\Gamma^2]}.\end{aligned} \tag{20}$$

Figure 8 shows the cross sections $\langle\sigma_{\rm dir}\rangle$ and $\langle\sigma_{\rm int}\rangle$ and the total cross section $\langle\sigma_{\rm at}\rangle$ averaged over the molecular orientation. The simulations were performed using Eqs. (14) and (20). Due to the polarization selectivity of the core excitation $(\mathbf{e}\cdot\mathbf{d}_{0c})\propto\cos\theta$, the orientational dephasing does not wash out the YDSE interference and the WPI, which manifested in a nicely resolved Doppler doublet (Fig. 8). This effect was observed for the first time in the RAS from oxygen molecules [22].

Figures 9 and 10 show that the orientational dephasing transforms the complementarity equations (4) and (7) to the correspondent inequalities

$$\overline{\mathcal{W}}+\overline{\mathcal{I}}<1, \quad \overline{\mathcal{W}}_{\rm GY}^2+\overline{\mathcal{I}}^2<1.$$

The Doppler labeling of the atomic slits is quenched in the regions $|\Delta E|\gg kv$ and $|\Delta E|\ll kv$ and takes the maximum at $\Delta E\approx\pm kv$. In full agreement with our present definition of the WPI, Eqs. (1) and (19), the results of simulations show the

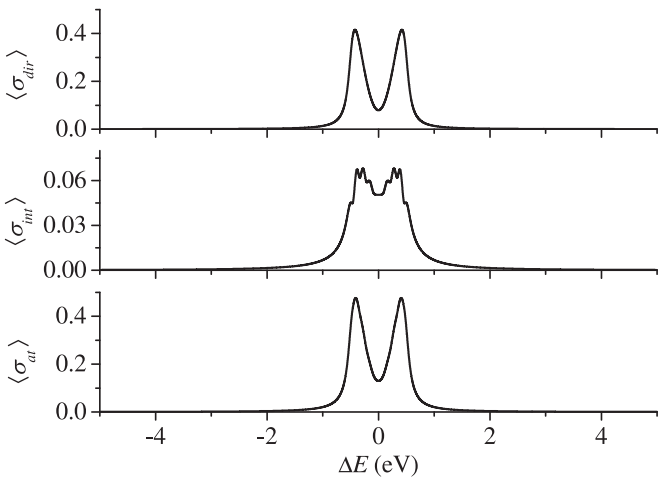

FIG. 8. Direct $\langle\sigma_{\rm dir}\rangle$, interference $\langle\sigma_{\rm int}\rangle$, and total $\langle\sigma_{\rm at}\rangle$ RAS cross sections averaged over molecular orientations. Calculations are performed using Eqs. (14) and (20).

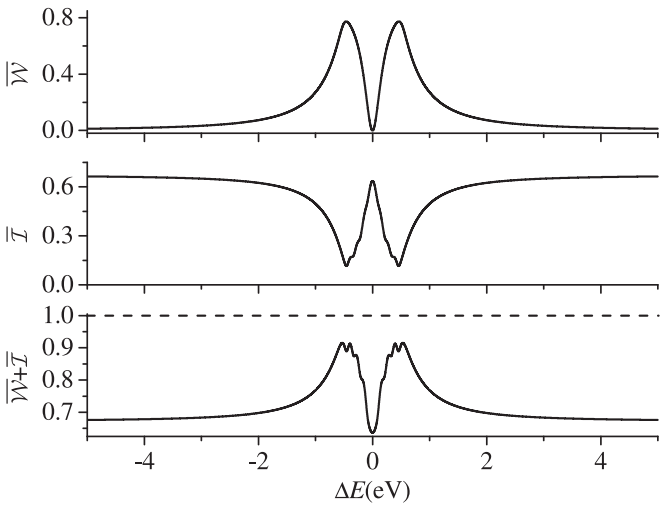

FIG. 9. Role of the orientational dephasing. Which-path information $\overline{\mathcal{W}}$, interference $\overline{\mathcal{I}}$, and $\overline{\mathcal{W}}+\overline{\mathcal{I}}$ averaged over the molecular orientations. Simulations are performed using Eq. (19).

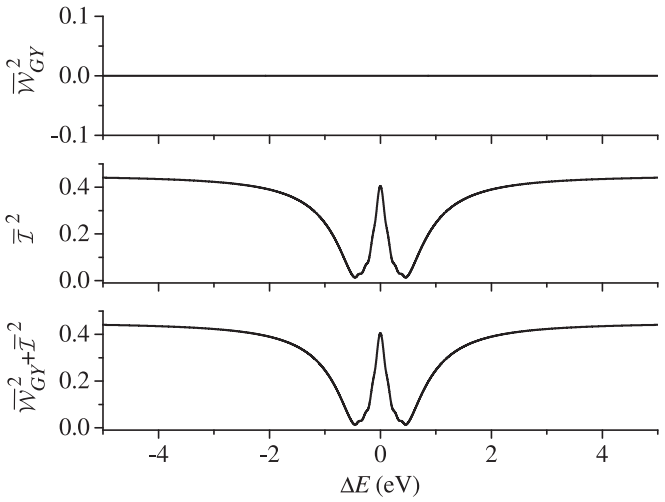

FIG. 10. Role of the orientational dephasing for GY's WPI definition. Simulations performed using Eq. (19). GY's WPI is strictly equal to zero for all ΔE contrary to our WPI definition shown in Fig. 9, where $\overline{\mathcal{W}} \neq 0$ except for $\Delta E = 0$ and $|\Delta E| \to \infty$.

maximum of $\overline{\mathcal{W}}$ near $\Delta E \approx \pm kv$ (Fig. 9). The interference $\mathcal{I}$ displays the opposite dependence on ΔE: It is suppressed near $\Delta E \approx \pm kv$ where the WPI is available (Figs. 9 and 10).

In contrast to our definition of the WPI given in this paper ($\overline{\mathcal{W}} \neq 0$, Fig. 9), the GY's WPI definition [Eqs. (5) and (19)] shows the rather unexpected result that the WPI is identically equal to zero (Fig. 10),

$$\overline{\mathcal{W}}_{\mathrm{GY}} \equiv 0,$$

despite that the path information is available due to the Doppler labeling of the atomic slits, as it was discussed above and observed in the experiment [22]. GY's path information $\overline{\mathcal{W}}_{\mathrm{GY}}$ is equal to zero because of the strict equality that is valid for the RAS process studied here:

$$\left\langle \left| F_{\mathrm{R}}^{(\mathrm{at})} \right|^2 \right\rangle \equiv \left\langle \left| F_{\mathrm{L}}^{(\mathrm{at})} \right|^2 \right\rangle.$$

Nevertheless, even with the above equality, the expectation value of the cross term for the RAS process in $\overline{\mathcal{W}}$ (19) is not equal to one,

$$\frac{2\left\langle \left| F_{\mathrm{R}}^{(\mathrm{at})} \right| \left| F_{\mathrm{L}}^{(\mathrm{at})} \right| \right\rangle}{\left\langle \left| F_{\mathrm{R}}^{(\mathrm{at})} \right|^2 + \left| F_{\mathrm{L}}^{(\mathrm{at})} \right|^2 \right\rangle} \neq 1,$$

and hence, $\overline{\mathcal{W}} \neq 0$, since $|F_{\mathrm{R}}^{(\mathrm{at})}| \neq |F_{\mathrm{L}}^{(\mathrm{at})}|$ due to the opposite Doppler shifts for right and left dissociating atoms.

Apparently this drawback of GY's definition of the WPI is not general property of $\overline{\mathcal{W}}_{\mathrm{GY}}$. This happens only for the studied here case of the RAS process with a rather specific Doppler labeling of the atomic slits in the randomly oriented molecular ensemble. In most cases, GY's definition of the WPI describes correctly the two-slit experiments with different origins of the path information.

V. CONCLUSIONS

In conclusion, we have obtained a different quantitative formulation of Bohr's complementarity for the pair which-path information and interference. We applied this principle for the analysis of resonant Auger scattering experiments performed with fixed-in-space and randomly oriented homonuclear molecules core-excited to the dissociative state. In spite of the short lifetime of the core-excited state, the molecule has time to dissociate. Auger decay of the dissociated core-excited atom results in a formation of a narrow, so-called atomic peak. Since the core-excited state is the intermediate one in the scattering process, the coherent scattering channels through the right and left atomic sites are indistinguishable and thus interfere. This phenomenon resembles strongly the YDSE interference except that the ultrafast dissociation brings the Doppler labels for the right and left counterpropagating atomic slits. The opposite Doppler shifts for dissociating atoms provide the which-path information.

We computed the which-path information, the interference, and their sum as functions of the angle of ejection of the Auger electron as well as their dependence on the kinetic energy of the Auger electron. In an agreement with Bohr's complementarity, this sum is smaller or equal to 1 for fixed-in-space molecules. The orientational dephasing in the case of the RAS with the randomly oriented molecular ensemble makes the sum smaller than 1. In an agreement with the complementarity principle the path information and the interference display opposite dependencies, the larger the which-path information the smaller the interference and vice versa. We did also the comparison of our quantitative formulation of the complementarity with the alternative formulation made earlier by Greenberger and Yasin [13]. Our and GY's formulations of the complementarity give qualitatively the same results for oriented molecules in contrast to the YDSE experiment with the randomly oriented molecules where the GY's path information is identically equal to zero in spite of the path information being available due to the Doppler labeling of the atomic slits.

ACKNOWLEDGMENTS

The research leading to obtained results has received funding from the Swedish Research Council (Project No. 2019-03470), the Ministry of Science and Higher Education of Russian Federation (Project No. FSRZ 2023-0006), the National Natural Science Foundation of China (Grants No. 11974108 and No. 12211530044), the Fundamental Research Funds for the Central Universities (Grant No. 2023JC005), and STINT Mobility Grants for Internationalisation (Project No. MG2021-9085). The computations were enabled by resources provided by the National Academic Infrastructure for Supercomputing in Sweden (NAISS) at PDC and NSC partially funded by the Swedish Research Council through Grants No. 2022-06725 and No. 2018-05973.

[1] N. Bohr, in *A. Einstein, Philosopher-Scientist*, edited by P. A. Schilpp (The Library of Living Philosophers, Evanston, 1949).

[2] W. Heisenberg, Über den anschaulichen inhalt der quantentheoretischen kinematik und mechanik, Z. Phys. **43**, 172 (1927).

[3] T. Young, The Bakerian lecture: Experiments and calculation relative to physical optics, Philos. Trans. R. Soc. London **94**, 1 (1804).

[4] F. Gel'mukhanov and H. Ågren, Resonant inelastic x-ray scattering with symmetry-selective excitation, Phys. Rev. A **49**, 4378 (1994).

[5] D. Mills, J. A. Sheehy, T. A. Ferrett, S. H. Southworth, R. Mayer, D. W. Lindle, and P. W. Langhoff, Nondipole resonant x-ray Raman spectroscopy: Polarized inelastic scattering at the K edge of Cl_2, Phys. Rev. Lett. **79**, 383 (1997).

[6] X.-J. Liu, N. A. Cherepkov, S. K. Semenov, V. Kimberg, F. Gel'mukhanov, G. Prümper, T. Lischke, T. Tanaka, M. Hoshino, H. Tanaka, and K. Ueda, Young's double-slit experiment using core-level photoemission from N_2: Revisiting Cohen-Fano's two-centre interference phenomenon, J. Phys. B: At., Mol. Opt. Phys. **39**, 4801 (2006).

[7] A. Revelli, M. Moretti Sala, G. Monaco, P. Becker, L. Bohatý, M. Hermanns, T. C. Koethe, T. Fröhlich, P. Warzanowski, T. Lorenz, S. V. Streltsov, P. H. M. van Loosdrecht, D. I. Khomskii, J. van den Brink, and M. Grüninger, Resonant inelastic x-ray incarnation of Young's double-slit experiment, Sci. Adv. **5**, eaav4020 (2019).

[8] J.-C. Liu, J. Wang, N. Ignatova, P. Krasnov, F. Gel'mukhanov, and V. Kimberg, Role of the Cohen-Fano interference in recoil-induced rotation, J. Chem. Phys. **158**, 114304 (2023).

[9] F. Gel'mukhanov, J.-C. Liu, P. Krasnov, N. Ignatova, J.-E. Rubensson, and V. Kimberg, Nonlocal resonant inelastic x-ray scattering, Phys. Rev. A **108**, 052820 (2023).

[10] J. Söderström, A. Ghosh, L. Kjellsson, V. Ekholm, T. Tokushima, C. Såthe, N. Velasquez, M. Simon, O. Björneholm, L. Duda, A. Naves de Brito, M. Odelius, J.-C. Liu, J. Wang, V. Kimberg, M. Agåker, J.-E. Rubensson, and F. Gel'mukhanov, Parity violation in resonant inelastic soft x-ray scattering at entangled core holes, Sci. Adv. **10**, eadk3114 (2024).

[11] O. Nairz, M. Arndt, and A. Zeilinger, Quantum interference experiments with large molecules, Am. J. Phys. **71**, 319 (2003).

[12] S. Eibenberger, S. Gerlich, M. Arndt, M. Mayor, and J. Tüxen, Matter-wave interference with particles selected from a molecular library with masses exceeding 10000 amu, Phys. Chem. Chem. Phys. **15**, 14696 (2013).

[13] D. M. Greenberger and A. Yasin, Simultaneous wave and particle knowledge in a neutron interferometer, Phys. Lett. A **128**, 391 (1988).

[14] B.-G. Englert, Remarks on some basic issues in quantum mechanics, Z. Naturforsch., A: Phys. Sci. **54**, 11 (1999).

[15] B.-G. Englert, Fringe visibility and which-way information: An inequality, Phys. Rev. Lett. **77**, 2154 (1996).

[16] A. Bramon, G. Garbarino, and B. C. Hiesmayr, Quantitative complementarity in two-path interferometry, Phys. Rev. A **69**, 022112 (2004).

[17] K. K. Menon and T. Qureshi, Wave-particle duality in asymmetric beam interference, Phys. Rev. A **98**, 022130 (2018).

[18] D.-X. Chen, Y. Zhang, J.-L. Zhao, Q.-C. Wu, Y.-L. Fang, C.-P. Yang, and F. Nori, Experimental investigation of wave-particle duality relations in asymmetric beam interference, npj Quantum Inf. **8**, 101 (2022).

[19] F. Gel'mukhanov, M. Odelius, S. P. Polyutov, A. Föhlisch, and V. Kimberg, Dynamics of resonant x-ray and Auger scattering, Rev. Mod. Phys. **93**, 035001 (2021).

[20] X.-J. Liu, Q. Miao, F. Gel'mukhanov, M. Patanen, O. Travnikova, C. Nicolas, H. Ågren, K. Ueda, and C. Miron, Einstein-Bohr recoiling double-slit gedanken experiment performed at the molecular level, Nat. Photon. **9**, 120 (2015).

[21] F. Gel'mukhanov and H. Ågren, Resonant x-ray Raman scattering, Phys. Rep. **312**, 87 (1999).

[22] O. Björneholm, M. Bässler, A. Ausmees, I. Hjelte, R. Feifel, H. Wang, C. Miron, M. N. Piancastelli, S. Svensson, S. L. Sorensen, F. Gel'mukhanov, and H. Ågren, Doppler splitting of in-flight Auger decay of dissociating oxygen molecules: The localization of delocalized core holes, Phys. Rev. Lett. **84**, 2826 (2000).

[23] J. Stöhr, *The Nature of X-Rays and Their Interactions with Matter*, 1st ed. (Springer, Berlin, 2023).

[24] J.-I. Adachi, N. Kosugi, and A. Yagishita, Symmetry-resolved soft X-ray absorption spectroscopy: its application to simple molecules, J. Phys. B: At., Mol. Opt. Phys. **38**, R127 (2005).

[25] M. N. Piancastelli, T. Marchenko, R. Guillemin, L. Journel, O. Travnikova, I. Ismail, and M. Simon, Hard x-ray spectroscopy and dynamics of isolated atoms and molecules: A review, Rep. Prog. Phys. **83**, 016401 (2020).

[26] F. Gel'mukhanov, H. Ågren, and P. Sałek, Doppler effects in resonant X-ray Raman scattering, Phys. Rev. A **57**, 2511 (1998).

[27] P. Sałek, F. Gel'mukhanov, H. Ågren, O. Björneholm, and S. Svensson, Generalized Franck-Condon principle for resonant photoemission, Phys. Rev. A **60**, 2786 (1999).

[28] P. Sałek, F. Gel'mukhanov, and H. Ågren, Wave packet dynamics of resonant x-ray Raman scattering excitation near the Cl $L_{II,III}$ edge of HCl, Phys. Rev. A **59**, 1147 (1999).